

# INFLUENCE OF INSUFFICIENTLY EMBEDDED MECHANICAL SPLICES ON MECHANICAL BEHAVIOR OF RC MEMBERS

Dac Phuong NGUYEN<sup>\*1</sup> and Hiroshi MUTSUYOSHI<sup>\*2</sup>

## ABSTRACT

Mechanical splices are sometimes installed incorrectly in a construction site when the centers of two steel bars are deviated. As a result, the steel bars are not embedded sufficiently in a coupler. RC members using such mechanical splices cannot achieve properties as expected. This paper shows mechanical behavior of such mechanical splices and RC beams using them. A numerical model for analyzing RC members using insufficiently embedded mechanical splices is also presented. The developed model, which bases on the well-known fiber model, is validated using the experimental results.

**Keywords:** reinforced concrete, mechanical splices, fiber model

## 1. INTRODUCTION

Nowadays, mechanical splices are very popular in construction of RC structures [1, 2]. As a matter of fact, mechanical splices are sometimes installed incorrectly. For example, in the fabrication of precast RC structures, the axes of the two bars often do not align exactly and the mechanical splices cannot be assembled properly as shown in Fig.1.

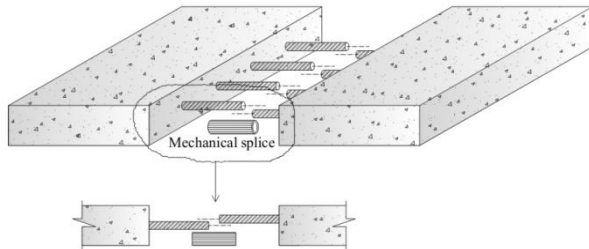


Fig.1 Example of insufficiently embedded mechanical splice in construction

There have been concerns that mechanical splices with insufficient embedment in the coupler may not have the required strength and it is very dangerous for a RC member using them. The objective of this study is to clarify properties of such mechanical splices and RC members. This study also develops a numerical model based on well-known fiber model that can analysis the behavior of RC members using insufficiently embedded mechanical splices.

## 2. INSUFFICIENTLY EMBEDDED MECHANICAL SPLICES IN JAPAN

To check for insufficient embedment of bars in mechanical splice couplers, random samplings of splices are carried out at construction sites in Japan using non-destructive ultrasonic testing methods (NDT). The basic principle of the NDT method is

using high frequency sound energy to conduct examinations and make measurements. Fig.2 shows the result of investigation of mechanical splices in construction sites conducted by Japan Reinforcing Bar Joints Institute. As can be seen, there are 4.4% insufficient insertion length mechanical splices out of 338 splices investigated.

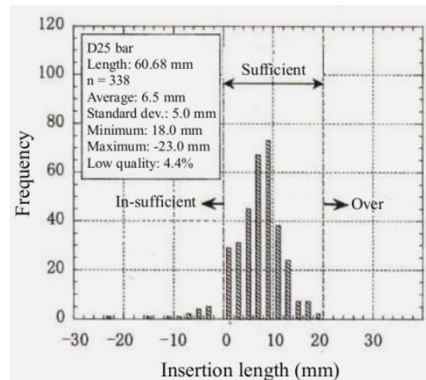


Fig.2 Investigation of insufficiently embedded mechanical splices

Number of insufficiently embedded mechanical splices is noticeable. Therefore, it is important to understand properties of such mechanical splices as well as their effect on behavior of RC members.

## 3. EXPERIMENTAL STUDY OF INSUFFICIENTLY EMBEDDED MECHANICAL SPLICES

### 3.1 Tensile test

Tensile tests were carried out to clarify properties of insufficiently embedded mechanical splices. The steel bar used in the tests was D19 bar. Four types of mechanical splices were prepared changing bar embedment lengths in the coupler and the existence of epoxy in the coupler. Fig.3 shows the configuration and detail of the specimens.

\*1 Postdoctoral Researcher, Graduate School of Science and Engineering, Saitama University, JCI Member  
 \*2 Professor, Graduate School of Science and Engineering, Saitama University, JCI Member

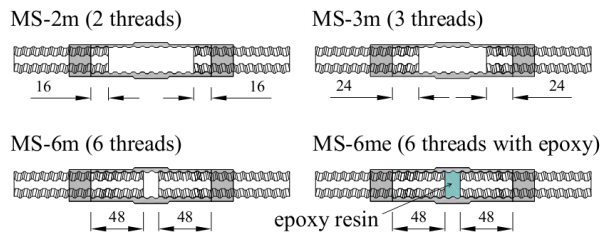


Fig.3 Tensile test specimens

Fig.4 shows the stress versus apparent strain curves of the specimens. The apparent strain of each mechanical splice is obtained by dividing the elongation of the splice section by its original length (180 mm including the mechanical splice).

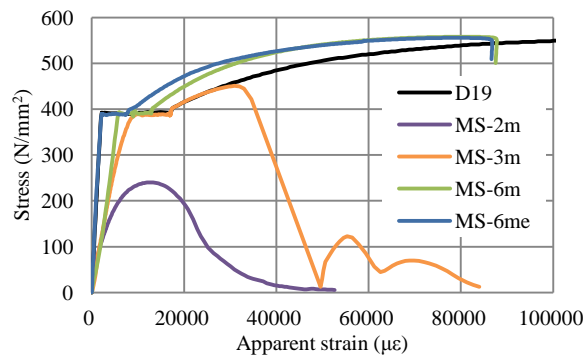


Fig.4 Stress-apparent strain curves

As can be seen, excepting the perfect mechanical splice MS-6me (fully embedded and injected epoxy), the other specimens have lower performance compared to the D19 bar. MS-2m and MS-3m have lower stiffness and strength, MS-6m has lower stiffness. All specimens failed at lower elongation compared to that of the D19 bar due to higher stiffness of the mechanical splice region.

Failure mode of insufficiently embedded mechanical splices (MS-2m and MS-3m) is slip out of the bar from the coupler. Sufficiently embedded mechanical splices (MS-6m and MS-6me) failed in the steel bars outside the coupler and therefore the strength at the failure showed the same one as the D19 bar.

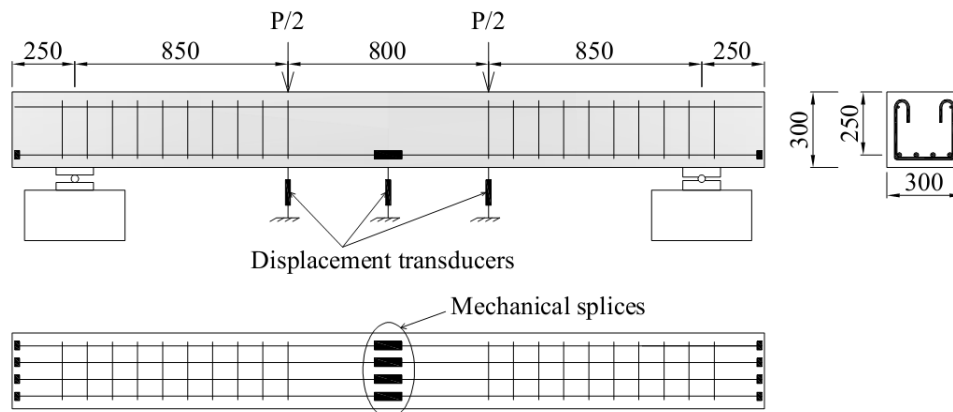


Fig.5 Beam dimensions and test set up (all measurements in mm)

### 3.2 RC beams using insufficiently embedded mechanical splices

#### (1) Specimen

Five RC beams were prepared changing insertion length of mechanical splices. All beams were 3 m length with a span of 2.5 m and 300 mm square cross section. Fig.5 shows the dimension of the test beams. The beams were longitudinally reinforced by four D19 steel bars and transversely reinforced in the shear span by D10 stirrups with 100 mm spacing. Mechanical splices were located at the center of the span. No stirrup was used in the moment constant span in order not to disturb the crack patterns. Summary of the test beams is shown in Table 1.

Table 1. Summary of the test beams

Beam	Mechanical splice type	Concrete strength (MPa)
B1	-	36.2
B2-2m	MS-2m	38.3
B3-3m	MS-3m	36.8
B4-6m	MS-6m	33.8
B5-6me	MS-6me	31.5

Electrical strain gages were used to measure the strains of reinforcement bars in the pure flexural region as well as the strains of concrete at the extreme compression surface at the mid span. Displacement transducers were used to measure the deflections of beams at the mid span and at two points of applied loads. The crack patterns were investigated and crack widths were measured along pure flexural region by using PI-shape displacement transducers. All data were recorded by using a data acquisition system.

The beams were tested cyclically. The load was applied by an actuator with a maximum capacity of 300 kN. At first, load was applied with 30 cycles for each of load amplitudes: 0.5 $P_{sy}$ , 0.7 $P_{sy}$  and 0.95 $P_{sy}$  ( $P_{sy}$ : calculated yield load). After yielding of the beam, the test was continued until failure.

(2) Test results

Fig.6 shows the load – displacement curves of the test beams. The control beam B1 shows the typical flexural load-displacement relationship. For the other beams using mechanical splices, when the applied load reached the cracking moment, flexural cracks occurred simultaneously at both ends of the mechanical splices due to smaller concrete cover in this region. The major flexural cracks appeared at the critical sections adjacent to the end of the mechanical splices and extended vertically by the increase of load followed by a drop in the applied load indicating a slipping of the steel bars from the mechanical splices. For further loading, number, width and extension of the cracks increased.

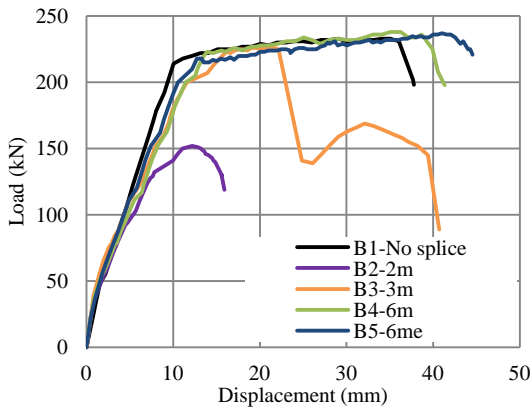


Fig.6 Load – displacement curves

Behavior of the beams using sufficient insertion length mechanical splices (B4, B5) is almost the same as the control beam. They could reach the same load carrying capacity as the control beam and failed in compression after reaching almost the same displacement. Thus, it was noticed that using sufficient insertion length mechanical splices had no significant influence on the bearing capacity and ductility compared to the beam using continuous bar.

The beam using MS-3m has the same load carrying capacity as the control beam while the ultimate displacement is smaller than that of the control beam. In this beam, the slip occurred thread by thread. Firstly, the steel bars slipped out one thread following by the sudden drop of load. After that the beam could bear some load before the failure.

In the beam using MS-2m, the reinforcing bars could not reach the yield strength because failure of the mechanical splices occurred prior to the yielding of the steel. The load carrying capacity of this beam is much smaller than that of the control beam. Failure mode of this beam was sudden and brittle.

4. ANALYSIS OF RC MEMBERS USING MECHANICAL SPLICES

4.1 Principle

Fiber model is one of the most promising models for analysis of RC members. It is a one-dimension, layer-by-layer approach. The RC

member is divided into longitudinal elements. There are numbers of control cross-sections located at the control points of the numerical integration scheme along the member. The characteristics of the member are obtained from integrating elements' sectional components along the member.

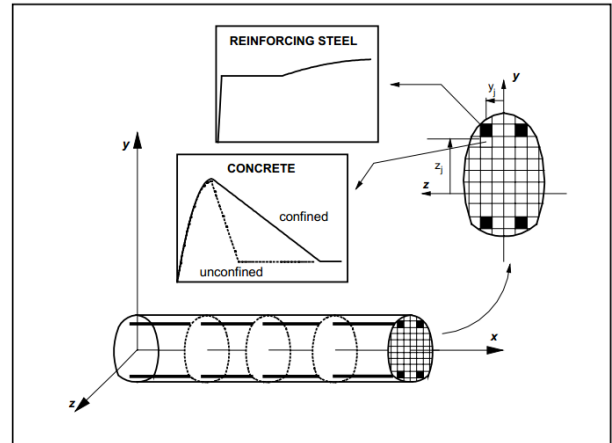


Fig.7 Principle of fiber model (F.Taucer et al.)

4.2 Material models

(1) Concrete

The monotonic envelope curve of concrete in compression follows the model of Kent and Park. It consists of a non-linear parabolic ascending part and a linear descending part as shown in Fig.8.

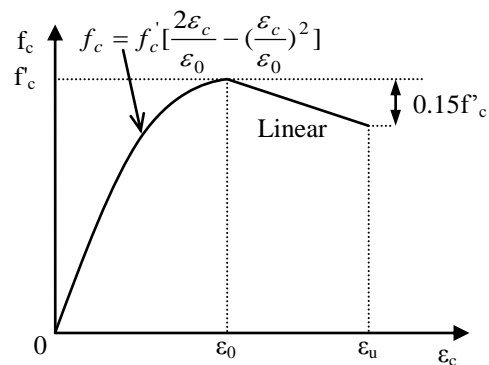


Fig.8 Concrete in compression

For concrete in tension, a linear stress-strain relationship is used (Fig.9).

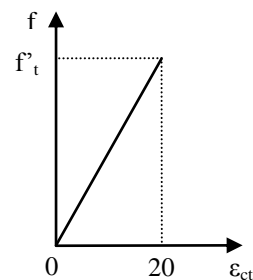


Fig.9 Concrete in tension

(2) Steel bars and mechanical splices

The tensile test results at yielding, hardening and ultimate stages are used to form the stress-strain relationships of the D19 bar and mechanical splices. These curves consist three portions: an initial elastic portion, a yield plateau, and a strain hardening portion up to failure.

4.3 Calculation procedure

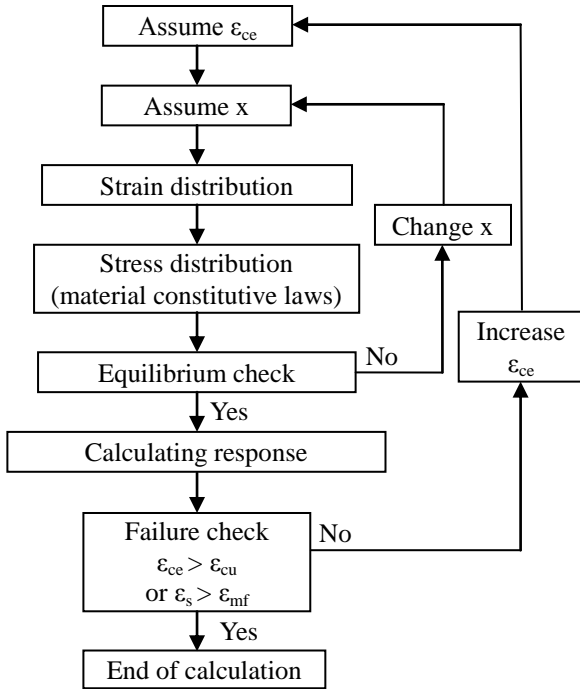


Fig.10 Calculation of M-φ of the section

For applying the fiber model to analyze a RC member using mechanical splices, the member is subdivided into 50-mm elements and the mechanical splice section is considered as one 180-mm element including the mechanical splice. The calculation

procedure is shown in Fig.10. To analyze the spliced section, deviation Δ in the stress-strain relationship between the mechanical splice and the reinforcing steel bar is calculated by following equation:

$$\Delta_\epsilon = \epsilon_m - \epsilon_s \tag{Eq.1}$$

where Δ<sub>ε</sub> = deviation at strain ε; ε<sub>m</sub> = strain of the mechanical splice; ε<sub>s</sub> = strain of the steel bar.

This procedure uses the stress-strain relationship of the steel bar in the calculation of sectional forces for both non-spliced and spliced sections. It is acceptable if based on an assumption that the small change in the neutral axis of the beam due to the deviation of using mechanical splices is neglected. The deviation Δ is taken into account when calculate curvature of the spliced-section:

$$\phi = \frac{\epsilon_{ce} + \epsilon_{se} + \Delta\epsilon}{h} \tag{Eq.2}$$

The calculation is finished when the strain at extreme compression fiber exceed the ultimate strain of the concrete or when the strain in the reinforcing bars ε<sub>s</sub> exceed the strain of the steel bars at the failure of the mechanical splices ε<sub>mf</sub>.

Load-displacement relation of the beam is calculated according to the procedure in Fig.11. Moment and curvature of the critical section are determined by the above procedure. The load producing this moment can be calculated and the moment along the member can be determined by using the moment diagram. On the other hand, the moment at each section can be also computed by using the section determination procedure of itself. The computed moment is compared with the determined moment and the strain at the extreme compression fiber is adjusted until the two values equal. By this way, the moment-curvature relationship of all the section is determined. The displacement of the member is then calculated by using the above formulas of rotation and displacement.

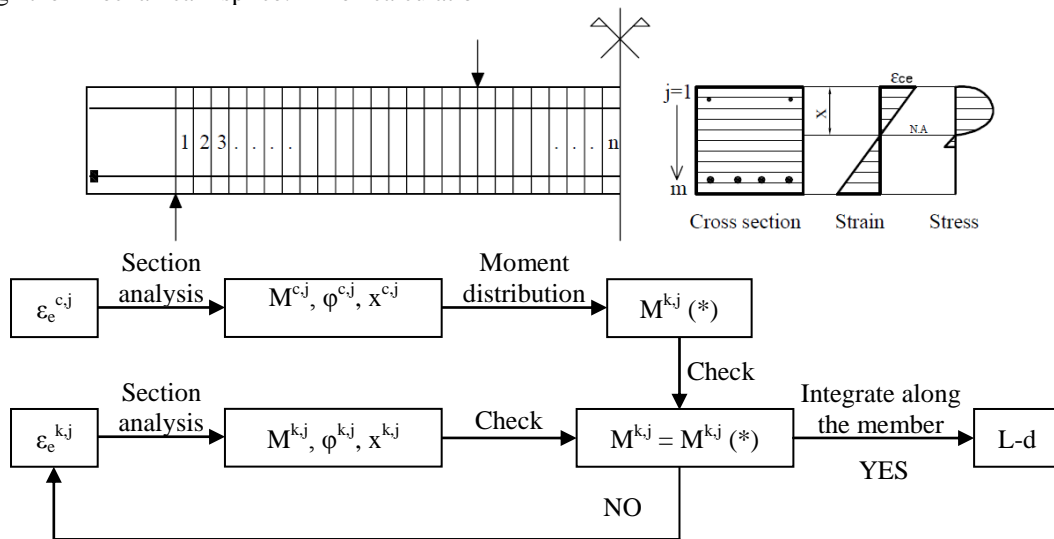


Fig.11 Calculation of L-d of the member

where “c” denotes for control section; ε<sub>e</sub> = strain at extreme fiber; M = moment; φ = curvature; x = neutral axis; L = applied load; d = deformation; j = 1, 2, ..., m (number of fibers of section); k = 1, 2, ..., n (number of elements).

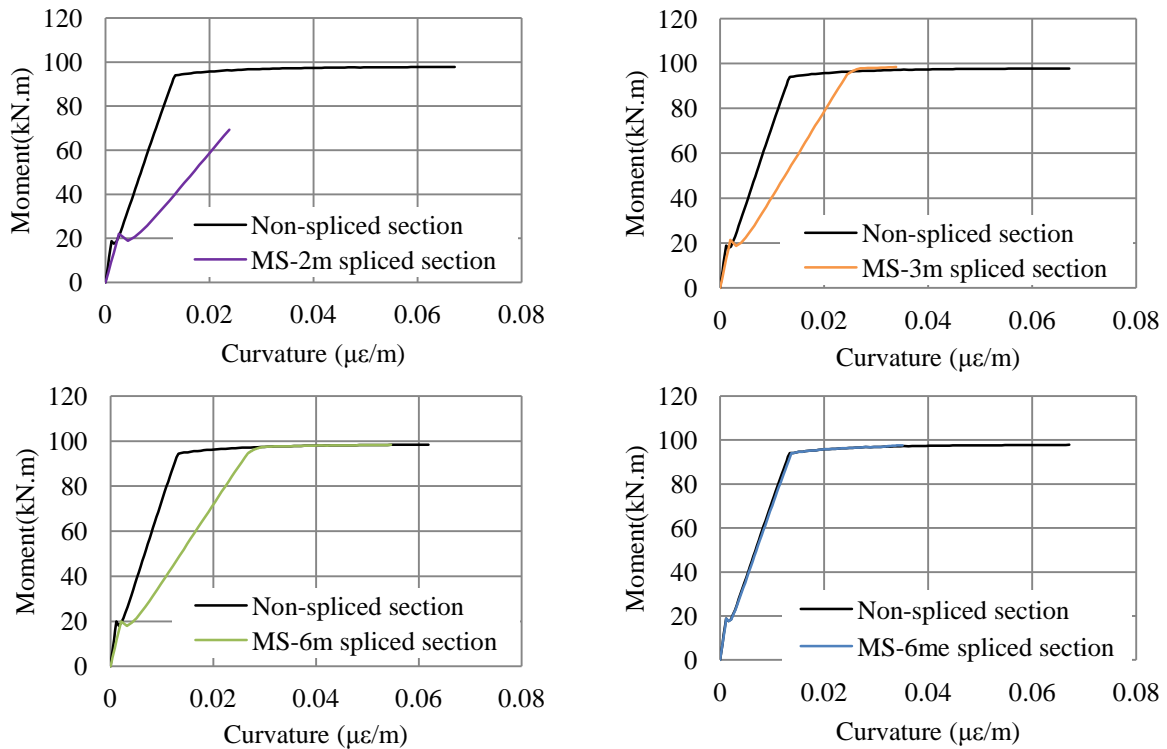


Fig.12 Calculated moment-curvature curves

#### 4.4 Analysis results and correlation with experimental results

##### (1) Moment-curvature of sections

Fig. 12 shows the moment-curvature curves obtained by the developed model. Before cracking, there is almost no difference between the moment-curvature curves of the spliced sections as compared to the non-spliced section. After cracking, it can be seen clearly the influence of mechanical splice quality on the moment-curvature relationship of the section. The M- $\phi$  curve of MS-2m spliced section has very low gradient and ultimate moment compared to those of the non-spliced section. The M- $\phi$  curve of MS-3m spliced section can reach the ultimate stage as the non-spliced section but with lower gradient. The M- $\phi$  curve of MS-6m spliced section has lower gradient compared to that of the non-spliced section. The M- $\phi$  curve of MS-6me spliced section has the same stiffness as that of the non-spliced section. All the spliced sections have lower ultimate curvature compared to that of the non-spliced section. The properties of these moment-curvature curves reflect well to the properties of the mechanical splice used (MS-2m, MS-3m, MS-6m and MS-6me).

##### (2) Load-deformation of beams

The calculated results of load-displacement of the beams by the developed model are correlated with the experimental results as shown in Fig.13. Obviously, the model has enough accuracy in

predicting behavior of the beams using mechanical splices. The failure mode is the same as in the experiments for all analyzed beams, as will be discussed in the following. Furthermore, the load-carrying capacity and stiffness agreed well for all beams.

Beam B2-2m failed suddenly and cannot reach the yielding stage. Beam B3-3m failed in bending due to yielding of tensile reinforcement. Both beams B2-2m and B3-3m using insufficiently embedded mechanical splices (MS-2m and MS-3m) failed at low ultimate displacement. The failure criteria of these two beams is  $\epsilon_s > \epsilon_{mf}$ , which means that the reinforcing bars were slipped out from the coupler. Beams B4-6m and B5-6me using sufficiently embedded mechanical splices (MS-6m and MS-6me) have almost the same load-carrying capacity and ultimate displacement as the control beam B1. The failure criteria of these two beams is  $\epsilon_{ce} > \epsilon_{cu}$ , which means that the beams failed due to crushing of concrete at the compression zone. The experimental curves of all beams are bent compared to the analyzed curves due to using the linearized stress-strain relationships of mechanical splices, not the tensile test results.

The developed model shows a good agreement with the experimental result. The assumption of using stress-strain relationship of the steel bar in the spliced section and the addition of deviation  $\Delta$  in calculating of curvature of the spliced section are able to simulate the behavior of RC members using mechanical splice.

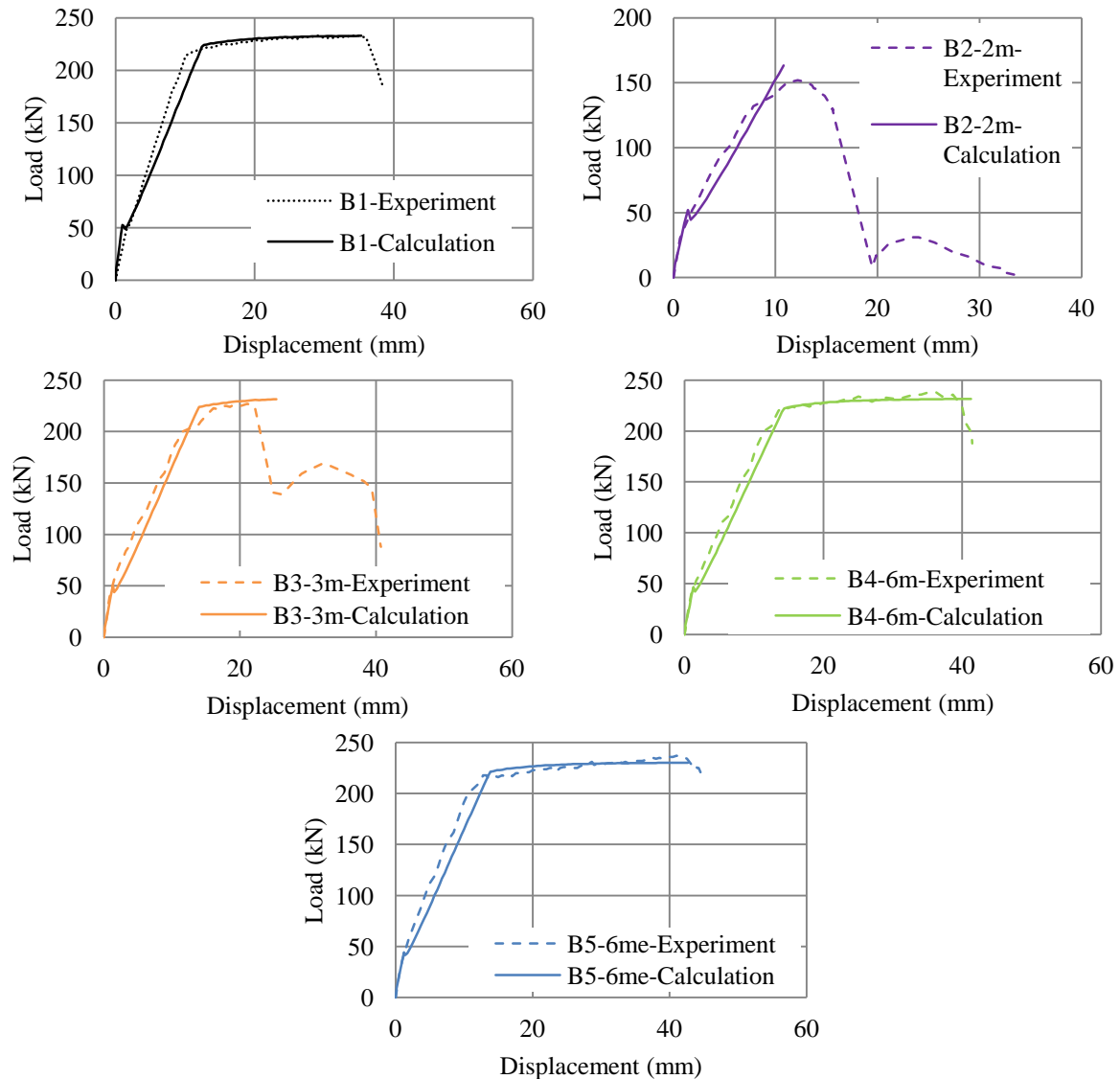


Fig.13 Load-displacement curves, experiment vs. analysis

## 5. CONCLUSIONS

Mechanical splices with different insertion lengths of the steel bar in the coupler and RC beams using them were tested. A theoretical model to predict the behavior of RC beams using mechanical splices had been developed based on the fiber model. The following conclusions can be drawn:

- (1) Insufficiently embedded mechanical splices have low performance on strength, stiffness and elongation.
- (2) RC beams using insufficiently embedded mechanical splices behave in dangerous manner due to slippage of steel bar from the coupler.
- (3) The developed fiber model is proved to be efficient to analyze the behavior of RC members using mechanical splices.

## ACKNOWLEDGEMENT

This study was supported by Grant-in-Aid for Scientific Research (B). The authors would like to

acknowledge members of Structural Material Laboratory of Saitama University for their help during the experimental works.

## REFERENCES

- [1] Japan Reinforcing Bar Joints Institute, "Standard Specification for Splice of Steel Bars – Mechanical Splice", 2009.
- [2] ACI Committee 439, "Types of Mechanical Splices for Reinforcing Bars", American Concrete Institute, March 2007.
- [3] Fabio F.Taucer, Enrico Spacone and Filip C.Filippou, "A Fiber Beam-Column Element for Seismic Response Analysis of Reinforced Concrete Structures", Research Report, 1991.
- [4] Amit H. Varma, Richard Sause, James M. Ricles, and Qinggang Li, "Development and Validation of Fiber Model for High-Strength Square Concrete-Filled Steel Beam-Columns Tube", ACI Structural Journal, V. 102, No. 1, January-February 2005, pp. 73-84.